

Cluster-and-Conquer: A Framework for Time-Series Forecasting

Reese Pathak¹ Rajat Sen² Nikhil Rao³ N. Benjamin Erichson^{4,5}
 Michael I. Jordan^{1,5} Inderjit S. Dhillon^{3,6}

¹Department of Electrical Engineering and Computer Sciences, UC Berkeley

²Google Research

³Amazon

⁴School of Engineering, University of Pittsburgh

⁵Department of Statistics, UC Berkeley

⁶Department of Computer Science, UT Austin

October 28, 2021

Abstract

We propose a three-stage framework for forecasting high-dimensional time-series data. Our method first estimates parameters for each univariate time series. Next, we use these parameters to cluster the time series. These clusters can be viewed as multivariate time series, for which we then compute parameters. The forecasted values of a single time series can depend on the history of other time series in the same cluster, accounting for intra-cluster similarity while minimizing potential noise in predictions by ignoring inter-cluster effects. Our framework—which we refer to as “cluster-and-conquer”—is highly general, allowing for any time-series forecasting and clustering method to be used in each step. It is computationally efficient and embarrassingly parallel. We motivate our framework with a theoretical analysis in an idealized mixed linear regression setting, where we provide guarantees on the quality of the estimates. We accompany these guarantees with experimental results that demonstrate the advantages of our framework: when instantiated with simple linear autoregressive models, we are able to achieve state-of-the-art results on several benchmark datasets, sometimes outperforming deep-learning-based approaches.

1 Introduction

High-dimensional time-series forecasting is crucial in applications such as finance [45], e-commerce [17], medical data analysis [31], fluid flows and climatology [13, 2]. Modern time-series datasets can have millions of correlated time series; e.g., demand forecasting for an online store like Amazon might require predicting the future sales of millions of items, and these demands are generally inter-related. Thus time-series forecasting methods should be scalable and equipped with the ability to handle inter-time-series correlation.

Most time-series forecasting methods operate at the two extremes: (1) **Univariate** modeling where the future prediction of a time series depends on its own past and associated covariates; (2) **Multivariate** modeling where the future prediction of a time series can potentially depend on the past of *all* the time series in the dataset. Univariate models are unable to capture inter time-series correlations during predictions, yet are computationally efficient and/or easy

to parallelize. On the other hand, multivariate time-series models are better able to capture these time-series correlations, yet can suffer from computational inefficiencies. We give a more extensive comparison of prior work within these two extremes, in Section 2.

The disadvantages of univariate and multivariate time-series modeling point to a need to come up with forecasting methods that can achieve a middle ground, i.e, the future values of a time series are modeled as a function of its own past and only a few other related time series. Therefore, in this paper we ask the following question: *For high-dimensional time-series problems, is it possible to develop statistically and computationally efficient methods that exploit only relevant inter-time-series relationships?* Prior works like [5] have indeed shown some promising empirical results in this direction, but detailed models of this problem with theoretical grounding is still lacking.

In this paper, we tackle this question in both theory and practice, and answer it in the affirmative. We propose a ‘cluster-and-conquer’ framework. Given n time series, we first use highly scalable univariate models (such as scalar autoregression) to learn parameters of each time series. Then, we apply efficient clustering algorithms on these parameters, to partition the collection of time series into k clusters. Finally, for each cluster, we apply a joint forecasting approach (using all the time series only in the cluster).

The *main contributions* of this paper are a framework for time-series modelling with the following properties:

- (i) By varying the number of clusters, we are able to interpolate between univariate and multivariate modelling, and reap the statistical and computational benefits of each paradigm.
- (ii) When employed with standard linear autoregressive models, our method shows strong empirical performance. Specifically, we are able to outperform many previously proposed time-series modelling approaches over a wide variety of datasets.
- (iii) Our framework—when analyzed in a mixture-of-regressions setting—enjoys theoretical guarantees. Namely, we can show that this framework is able to ensure recovery of model parameters at standard parametric rates.

Notation. A multivariate time-series dataset with n time series and T time points can be represented as $\mathbf{X} \in \mathbf{R}^{n \times T}$. For integers, $i \leq j$, $i : j := \{i, i + 1, \dots, j\}$. For a positive integer n , $[n]$ denotes the set $\{1, 2, \dots, n\}$. The notation $x_i^{(\mathcal{J})}$ denotes the values at the time points in \mathcal{J} for time series i represented as a column vector, in ascending order of the indices in \mathcal{J} . $\|\cdot\|_p$ denotes the ℓ_p norm for vectors. The operator and Frobenius norms of matrices are denoted by $\|\cdot\|_{\text{op}}$ and $\|\cdot\|_{\text{F}}$ respectively. For two vectors $u \in \mathbf{R}^p, v \in \mathbf{R}^q$, we write $u \otimes v$ for their tensor (outer) product, which is a $p \times q$ matrix with entries $u_i v_j, i \in [p], j \in [q]$.

2 Related Work

There is a vast body of work in classical time-series forecasting; we refer the reader to Hyndman and Athanasopoulos [21] for an overview. Here, we mainly focus on the time-series forecasting literature in the machine learning community; see also Benidis et al. [6].

Univariate modeling. Basic forecasting techniques train one model per dataset but the prediction using the trained model is done for each time series and its covariates individually.

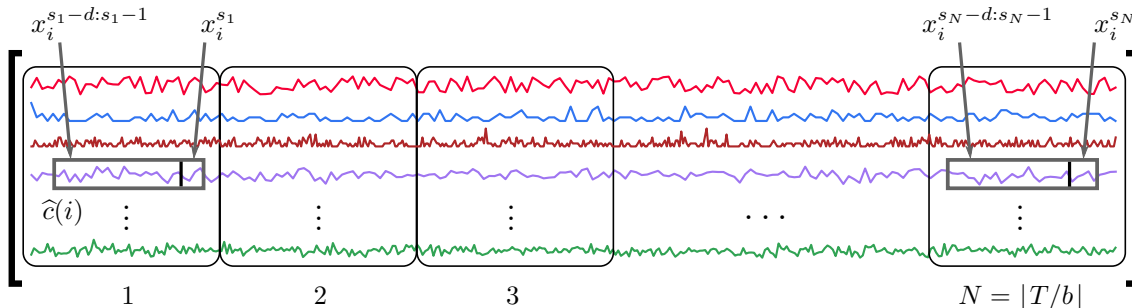


Figure 1: Illustration of forming regression datasets from time-series data blocks. Since b is a multiple of the mixing time of the time series, the samples for the regression problem will be approximately be independent and identically distributed. Above, $\{s_i\}_{i=1}^N$ are the sample time points selected within each chunk.

Specifically, in univariate modeling, we typically use predictions of the form

$$\hat{x}_i^{(T+1)} = \hat{f}_i(x_i^{(1:T)}), \quad i = 1, \dots, n.*$$

Autoregressive (AR) models are a classic example that are computationally scalable and enjoy low variance, but these models typically suffer from high statistical bias in that they cannot account for complicated inter-time-series relationships. In contrast, recent deep learning methods [35, 8, 15, 29, 34] aim to address this problem by training shared weights of a large model on the whole dataset—effectively selecting \hat{f}_i based on the other time series $\{x_i^{(t)}\}_{t \leq T, j \neq i}$. At prediction time the estimate of future values of each univariate time series is modelled by a function of its own past and covariates.

Multivariate modeling. More advanced forecasting techniques aim to capture dependencies across different time series in the dataset. Prediction for each time series is computed as a function of the history of *all* the other time series. Specifically, in multivariate modeling, we typically use predictions of the form

$$\hat{x}_i^{(T+1)} = \hat{f}_i(x_1^{(1:T)}, x_2^{(1:T)}, \dots, x_n^{(1:T)}).$$

Models that use this paradigm include dense vector autoregression (VAR), dynamic linear models (DLMs), TRMF [43], DeepGLO [36] and graph neural network based models [28, 9, 42, 40, 20, 3, 14]. However, some of these models are computationally inefficient. For instance, VAR does not scale beyond even moderately sized datasets. The complexity to fit a VAR model on a dataset of n time series scales as $O(n^6)$ [43]. Similarly, DLMs typically scale as $O(n^3)$, which is again prohibitive for large- n problems. Additionally, these models typically have a large number of parameters, and can therefore suffer from high model variance. At prediction time, forecasts can be made using contributions from potentially irrelevant time series which can lead to higher statistical error.

Time-series clustering. The vast literature on time-series clustering is also relevant to our work. We refer the reader to the surveys by Warren Liao [39] and Aghabozorgi et al. [1] for

*We use \hat{x}, \hat{f} to denote estimates.

an in-depth treatment. Model-based clustering techniques that assume that similar time series are governed by similar model parameters are especially relevant to our work [22, 12, 38]. In recent work [5], Bandara and co-authors consider a similar cluster-based time-series prediction framework. However, there are two main differences: first, the authors do not present theory to justify or accompany their modelling framework. Secondly, their within-cluster model does not forecast individual time series based on the entire history of the other time series, and could miss important inter-cluster time-series correlations.

3 Cluster-and-Conquer Framework

Suppose we are given a history of T timepoints of n univariate time series, $\{x_i^{(t)}\}_{i \leq n, t \leq T}$. We would like to produce a prediction, for the next time point, which is at time $T + 1$.[†] We want our predictions to satisfy $\hat{x}_i^{(T+1)} \approx x_i^{(T+1)}$, for all time series $i = 1, \dots, n$. Now, to overcome some of the issues discussed in the related work section, we propose a three-stage procedure for time-series forecasting.

Our framework consists of the following three steps:

- **Local step:** We first divide the time-series dataset into $N = \lfloor T/b \rfloor$ chunks of contiguous times as shown in Figure 1; within each of the N chunks, we select a time point $s_i, i \in [N]$, for which we sample the data. At a high level, we can think of selecting b as a multiple of the (largest) mixing time of the time series. We can now extract one sample for a local autoregressive regression problem per time series from each block. For example for the i -th time series the sample from the j -th block can be

$$(\text{covariates}, \text{target}) = (x_i^{(s_j - d : s_j - 1)}, x_i^{(s_j)}).$$

For each time series we collect all the samples and solve a least-squares problem, and hence this step is efficient. The AR parameters obtained are $\{\hat{\theta}_i^{\text{AR}}\}_{i=1}^n$.

- **Clustering step:** Next, we cluster the parameters of the AR model. We can use a clustering algorithm, for instance spectral clustering [23], or METIS [22] with inputs $\{\hat{\theta}_i^{\text{AR}}\}_{i=1}^n$ to obtain a clustering of time series into k clusters. Let $\hat{c}(i)$ be the estimated cluster identity of time series i .
- **Global step:** Given a partition, we can estimate VAR parameters for every cluster. We can reuse the block structure from above and extract one sample per block for the VAR problem associated with each time series. For instance, for the i -th time series the sample for the j -th block can be

$$\begin{aligned} \text{covariates} &= x_i^{(s_j - d : s_j - 1)}, \{x_l^{(s_j - d : s_j - 1)}\}_{\hat{c}(l) = \hat{c}(i)}, \\ \text{target} &= x_i^{(s_j)}. \end{aligned}$$

The covariates are the history of the i th time series, together with all the histories of the time series assigned to the same cluster—that is, time series l satisfying $\hat{c}(l) = \hat{c}(i)$.

Therefore, in this model the future of a time series can depend on the past of all time

[†]For simplicity we write all our equations for predicting one time point in the future, however all the ideas trivially extend to multi-step forecasting.

series in the same cluster, through the learned VAR coefficients. Note that we use VAR here for exposition and to make it amenable to theoretical analysis. In practice, this step can be solved using more complex low-rank [43] or deep-learning [36] approaches.

Each of the samples for the two regression problems above should be close to i.i.d as b is a multiple of the mixing time of the processes. Therefore we will analyze an i.i.d analogue of the above system which is similar to a mixed linear regression problem. The mixed linear regression problem is a useful surrogate of our problem in an i.i.d setting that lets us analyze the salient features of our framework—parameter recovery of local AR models, recovery of clusters using clustering on the recovered AR parameters and recovery of VAR parameters within cluster—while avoiding the complexities arising from non-i.i.d data. Note that risk bounds and parameter recovery bounds for simple AR models are still an area of active research [19, 32, 25] and we would like to decouple the hardness of analyzing our framework from the issues arising from a non-i.i.d dataset. These issues can be carefully dealt with using tools from mixing time literature and are left for future work. Analogous i.i.d settings have been used before in the literature to analyze interesting properties of time-series clustering algorithms [38, 12].

4 Theoretical Results

In this section we provide our formal algorithm and associated parameter recovery guarantees in the Mixed Linear Regression (MLR) setting. Although idealized, this formal model allows us to state formal guarantees about parameter recovery. Additionally, we refer the reader to Appendix D.1, where we further explain how this setting is closely related to the original time-series problem.

MLR model: We consider the following fixed design mixed linear regression problem. There are n regression designs each with T samples. $x_i^{(t)}$ denotes the t -th covariate from the i -th design. We will use the notation $X^{(t)} = \{x_i^{(t)}\}_{i=1}^n$, where $X^{(t)} \in \mathbf{R}^{n \times d}$.

We assume that for some positive integer k , we have (unknown) cluster labels, $\mathbf{c}^*(1), \dots, \mathbf{c}^*(n) \in [k]^n$, for each regression problem, where for all $i \in [n], t \in [T]$:

$$\theta_i \stackrel{\text{i.i.d.}}{\sim} \mathbf{N}_d(\bar{\theta}_{\mathbf{c}^*(i)}, \nu^2 I_d).$$

We then observe $\{y_i^{(t)}\}_{i=1}^n$ for $t = 1, \dots, T$ according to the following linear observational model:

$$y_i^{(t)} = \theta_i^\top x_i^{(t)} + \sum_{\substack{j \neq i \\ \mathbf{c}^*(j) = \mathbf{c}^*(i)}} \gamma_{ij}^\top x_j^{(t)} + \varepsilon_i^{(t)}, \quad \text{for } i \in [n]. \quad (1)$$

For simplicity, we assume that

$$\varepsilon_i^{(t)} \stackrel{\text{i.i.d.}}{\sim} \mathbf{N}(0, \sigma^2) \quad \text{and} \quad \gamma_{ij} \stackrel{\text{i.i.d.}}{\sim} \mathbf{N}_d(0, \tau^2 I_d).$$

The target $y_i^{(t)}$ can be thought of as the future value of i th time series that needs to be predicted. It depends linearly on its own past $x_i^{(t)}$ and also the past of the other time series in the same cluster $\{x_j^{(t)}\}$. The local AR parameters θ_i for each cluster come from the same Gaussian distribution.

4.1 Algorithm for Mixed Linear Regression

Our framework for the mixed linear regression problem is instantiated as Algorithm 1.

Algorithm 1 *Cluster & Conquer for Mixed Linear Regression.*

input: $y_i^{(t)}, x_i^{(t)}$ for $i \in [n], t \in [T]$.

1. Train one AR model per time series $\{\widehat{\theta}_i^{(AR)}\}_{i=1}^n$, according to Equation (2).
 2. Estimate cluster indices $\{\widehat{c}(i)\}_{i=1}^n$ using Algorithm 2.
 3. Solve VAR models for each cluster as in (5).
-

4.2 Overview of Guarantees

We now analyze Algorithm 1 in the mixed linear regression setting defined in Section 4, under the following assumptions.

Assumption 1. The number of clusters $k \geq \rho n$ for some constant $\rho \in (0, 1)$.

Assumption 2. The cluster sizes are uniform: each cluster has $m = n/k$ time series associated to it.

Assumption 3. Within each cluster, the design is isotropic. More formally, for cluster $\iota \in [k]$, suppose that time series $i_1, \dots, i_m \in [n]$ belong to this cluster (i.e., $c^*(i_j) = \iota$ for $j \in [m]$). Define for each $t \in [T]$

$$x_\iota^{(t)} = (x_{i_1}^{(t)}, \dots, x_{i_m}^{(t)}) \in \mathbf{R}^{md}$$

Then we assume $\frac{1}{T} \sum_{t=1}^T x_\iota^{(t)} \otimes x_\iota^{(t)} = I_{md}$, for all $\iota \in [k]$.

Our analysis will aim to demonstrate that Algorithm 1 provides good estimates of the autoregression parameters. To do so, we begin in Section 4.3 by providing a stochastic decomposition for the scalar AR parameters estimated for each time series. Having done so, we will establish that the scalar AR parameters are nearly a Gaussian mixture model. We are then able to extend existing guarantees for Gaussian mixtures to our setting, giving explicit conditions under which we can exactly recover the cluster labels for the mixed linear regression model via spectral clustering on the scalar AR estimates. These guarantees are provided in Section 4.4. We then study the properties of a single cluster-wide vector autoregression, and provide a high probability bound on the errors incurred from model noise. By union bounding over the clusters and the failure probability in our exact clustering guarantee, we are able to give a formal statement on the recovery guarantees of Algorithm 1.

4.3 Scalar Autoregression

As the first step of our procedure we propose fitting scalar autoregression parameter estimates according to a $\text{AR}(d)$ model. Formally, we estimate $\widehat{\theta}_i^{\text{AR}} \in \mathbf{R}^d$, for $i \in [n]$ via the following empirical risk minimization problem,

$$\widehat{\theta}_i^{\text{AR}} := \arg \min_{\theta \in \mathbf{R}^d} \left\{ \frac{1}{T} \sum_{t=1}^T (\theta^\top x_i^{(t)} - y_i^{(t)})^2 \right\}. \quad (2)$$

Our analysis begins with a stochastic decomposition of $\widehat{\theta}_i^{\text{AR}}$. To state it, we introduce the following notation for the (weighted) empirical covariance matrix, for a given time series. For any weights $\rho = (\rho^{(1)}, \dots, \rho^{(T)}) \in \mathbf{R}^T$, we define

$$\widehat{\Sigma}_i(\rho) := \frac{1}{T} \sum_{t=1}^T \mathbb{T}(\rho^{(t)})^2 x_i^{(t)} \otimes x_i^{(t)}.$$

In the special case $\rho = \mathbf{1}$, we write $\widehat{\Sigma}_i := \widehat{\Sigma}_i(\mathbf{1})$. With this notation in hand, we can now state the decomposition mentioned above.

Lemma 1. *For each $i \in [n]$, we have $\widehat{\theta}_i^{\text{AR}} \stackrel{\text{i.i.d.}}{\sim} \mathbf{N}_d(\bar{\theta}_{c^*(i)}, \Lambda_i)$, where*

$$\Lambda_i := \nu^2 I_d + \frac{\sigma^2}{T} \widehat{\Sigma}_i^{-1} + \frac{\tau^2}{T} \widehat{\Sigma}_i^{-2} \widehat{\Sigma}_i(\rho_i),$$

where $\rho_i = (\rho_i^{(1)}, \dots, \rho_i^{(T)})$, with $\rho_i^{(t)} := \sqrt{\sum_{j: c^*(j) = c^*(i)} \|x_j^{(t)}\|_2^2}$, for $t \in [T]$.

Whereas the true AR parameters θ_i follow a Gaussian mixture model, Lemma 1 shows that $\widehat{\theta}_i^{\text{AR}}$, while not a Gaussian mixture due to the different covariances Λ_i , is at least centered at the cluster mean $\bar{\theta}_{c^*(i)}$ for each $i \in [n]$. The proof has been deferred to the appendix in Section B.

We note that under Assumption 3, the covariances above can be further simplified to

$$\Lambda_i := \left(\nu^2 + \frac{\sigma^2}{T} \right) I_d + \frac{\tau^2}{T} \widehat{\Sigma}_i(\rho_i). \quad (3)$$

This will be a useful identity in the sequel.

4.4 A Result for Near Mixtures of Gaussians

As we demonstrated in Lemma 1, after computing autoregression estimates $\widehat{\theta}_i^{\text{AR}}$, we obtain a near mixture of Gaussians. In order to obtain guarantees for the vector autoregression, we first show that the clustering estimates are consistent. We begin with the following general result for near mixtures of Gaussians.

Setting. To state the result, we begin by formally defining our setting. Suppose there are k clusters, and n data points $X_1, \dots, X_n \in \mathbf{R}^d$. These data are associated to unknown cluster labels $c^*(i)$, where we view $c^*: [n] \rightarrow [k]$ as the labelling function. We assume that there are unknown cluster centers, $\theta_1^*, \dots, \theta_k^* \in \mathbf{R}^d$. Further assume we observe

$$X_i \stackrel{\text{ind.}}{\sim} \mathbf{N}_d(\theta_{c^*(i)}^*, \Sigma_i), \quad i = 1, \dots, n.$$

We additionally assume that the sample covariances $\Sigma_1, \dots, \Sigma_n$ are unknown. Note that this is not quite a mixture of Gaussians, since we allow that $\Sigma_i \neq \Sigma_j$, even if $c^*(i) = c^*(j)$.

Clustering near Gaussian mixtures. We study the spectral clustering algorithm, Algorithm 2 and provide the following recovery guarantee for near mixture of Gaussians.

Theorem 1. *Suppose that $\Sigma_i \preceq \gamma I_d$, for $i \in [n]$. Suppose Assumption 1 holds. Assume that the centers are well separated:*

$$\min_{i \neq j \in [k]} \|\theta_i^* - \theta_j^*\|_2 \geq 32\sqrt{\gamma}k \sqrt{\frac{1 + \frac{d}{n}}{\beta}} \max\left\{1, \frac{\beta}{\rho}\right\}.$$

Then, with probability at least $1 - \exp(-0.08n)$, there exists a permutation $\phi: [k] \rightarrow [k]$ such that $\widehat{\mathbf{c}}_{\text{spec}}(i) = \phi(\mathbf{c}^*(i))$ for all $i \in [n]$.

The proof is presented in Section A of the appendix. The above theorem implies the following corollary for our mixture of regression problem.

Corollary 1. *Suppose that Assumptions 1, 2, and 3 hold. Let*

$$\lambda := \nu^2 + \frac{\sigma^2 + \frac{\tau^2}{\rho}}{T}.$$

If the following separation condition holds,

$$\min_{i \neq j \in [k]} \|\bar{\theta}_i - \bar{\theta}_j\|_2 \geq 32\sqrt{\lambda}k \sqrt{\frac{1 + \frac{d}{n}}{\beta}} \max\left\{1, \frac{\beta}{\rho}\right\},$$

then spectral clustering on $\{\widehat{\theta}_i^{\text{AR}}\}_{i=1}^n$ produces an estimate $\widehat{\mathbf{c}}_{\text{spec}}$ which is exactly equal to the true clustering \mathbf{c}^* (up to relabellings of $\{1, \dots, k\}$) with probability $1 - \exp(-0.08n)$.

Algorithm 2 [Spectral clustering] *Algorithm for estimating clusters from samples [23].*

input: sample matrix $X \in \mathbf{R}^{d \times n}$, number of clusters, k

1. Compute truncated SVD of sample matrix.

$$X_k := \sum_{i=1}^k \widehat{\sigma}_i \widehat{u}_i \widehat{v}_i^\top =: \widehat{U} \widehat{\Sigma} \widehat{V}^\top \in \mathbf{R}^{d \times n}$$

2. Compute projection onto top- k left singular vectors.

$$Y := \widehat{U}^\top X_k = \widehat{\Sigma} \widehat{V}^\top \in \mathbf{R}^{k \times n}$$

3. Solve k -means on the columns of Y . Solve:

$$\text{minimize } \frac{1}{2n} \sum_{i=1}^n \|Y_i - \eta_{\kappa_i}\|_2^2,$$

with variables $\eta_1, \dots, \eta_k \in \mathbf{R}^k$ and $\kappa_1, \dots, \kappa_n \in [k]$.

output: labelling $\widehat{\mathbf{c}}_{\text{spec}}: [n] \rightarrow [k]$, where $\widehat{\mathbf{c}}_{\text{spec}}(i) := \kappa_i^*$.

4.5 Vector Autoregression per Cluster

The final step of our argument requires us to compute a high-probability guarantee on the closeness of estimated vector autoregression parameters.

For each cluster $\iota \in [k]$, under Assumption 2, there is an index set,

$$\{j \in [n] : \mathbf{c}^*(j) = \iota\} = \{i_1, \dots, i_m\} \subset [n],$$

that specifies the indices of the time series that truly belong to cluster $\iota \in [k]$. Define the following vectorized data:

$$y_\iota^{(t)} = \begin{bmatrix} y_{i_1}^{(t)} \\ \vdots \\ y_{i_m}^{(t)} \end{bmatrix} \quad \text{and} \quad x_\iota^{(t)} = \begin{bmatrix} x_{i_1}^{(t)} \\ \vdots \\ x_{i_m}^{(t)} \end{bmatrix}.$$

Hence, $y_\iota^{(t)} \in \mathbf{R}^m$ and $x_\iota^{(t)} \in \mathbf{R}^{md}$, for $\iota \in [k]$ and $t \in [T]$.

With this notation in hand, for each cluster $\iota \in [k]$, the observational model stated in (1) is equivalent to

$$y_\iota^{(t)} = (I_m \otimes (x_\iota^{(t)})^\top) \Gamma_\iota^* + \varepsilon_\iota^{(t)}, \text{ for all } t \in [T], \iota \in [k].$$

Here we define $\Gamma_\iota^* \in \mathbf{R}^{m^2d}$ to be the concatenation of the parameters in cluster $\iota \in [k]$. Specifically, in view of our observational model (1), suppose that we define

$$\tilde{\gamma}_{i_u i_v} := \begin{cases} \theta_{i_u} & u = v \\ \gamma_{i_u i_v} & u \neq v \end{cases}, \quad \text{for } u, v \in [m].$$

Then

$$\Gamma_\iota^* = \left(\tilde{\gamma}_{i_1 i_1}, \tilde{\gamma}_{i_1 i_2}, \dots, \tilde{\gamma}_{i_2 i_1}, \tilde{\gamma}_{i_2 i_2}, \dots, \gamma_{i_m i_m} \right) \in \mathbf{R}^{m^2d}.$$

This is our target of estimation.

Oracle VAR estimator. The first estimator we study is what we refer to as the *oracle VAR estimate for cluster ι* :

$$\Gamma_\iota^{\text{VAR,or}} := \arg \min_{\Gamma \in \mathbf{R}^{m^2d}} \left\{ \frac{1}{2T} \sum_{t=1}^T \|y_\iota^{(t)} - (I_m \otimes (x_\iota^{(t)})^\top) \Gamma\|_2^2 \right\}. \quad (4)$$

Crucially, it assumes knowledge of the set $\{i_1, \dots, i_m\}$, which are those time series which truly belong to cluster $\iota \in [k]$.

For this estimator, we have the following guarantee.

Lemma 2. *Suppose that Assumption 3 holds. Then for each $\iota \in [k]$, with probability at least $1 - \delta$ we have*

$$\|\Gamma_\iota^{\text{VAR,or}} - \Gamma_\iota^*\|_2 \leq \sqrt{2} \sqrt{\frac{\sigma^2 m^2 d}{T}} + \sqrt{3 \frac{\sigma^2}{T} \log \frac{1}{\delta}}.$$

Deferring the proof to the appendix, an outline is as follows. First we demonstrate that under the stated assumptions, $\Gamma_i^{\text{VAR,or}} \sim \mathbf{N}(\Gamma_i^*, \frac{\sigma^2}{T} I_{m^2d})$. Consequently,

$$\mathbf{E} \left[\|\Gamma_i^{\text{VAR,or}} - \Gamma_i^*\|_2^2 \right] \leq \frac{\sigma^2 m^2 d}{T}.$$

Establishing concentration around the mean is a consequence of tail-bounds for χ^2 random variates. We provide the full proof in Section B of the appendix.

VAR estimator with estimated clustering. We will show that the preceding result and Corollary 1, immediately imply our main recovery guarantee, via a simple appeal to a union bound. To state this result, we first need to describe how to construct the VAR estimate when the ground truth clustering is unknown. To do this, we define the following index set:

$$\{j \in [n] : \widehat{\mathbf{c}}(j) = \iota\} = \{\widehat{i}_1, \dots, \widehat{i}_{m_\iota}\} \subset [n].$$

This is the set of time series which are estimated to belong to cluster ι . Define

$$\widehat{\mathbf{y}}_\iota^{(t)} = \begin{bmatrix} y_{\widehat{i}_1}^{(t)} \\ \vdots \\ y_{\widehat{i}_{m_\iota}}^{(t)} \end{bmatrix} \quad \text{and} \quad \widehat{\mathbf{x}}_\iota^{(t)} = \begin{bmatrix} x_{\widehat{i}_1}^{(t)} \\ \vdots \\ x_{\widehat{i}_{m_\iota}}^{(t)} \end{bmatrix}.$$

Hence, $\widehat{\mathbf{y}}_\iota^{(t)} \in \mathbf{R}^{m_\iota}$ and $\widehat{\mathbf{x}}_\iota^{(t)} \in \mathbf{R}^{m_\iota d}$, for $\iota \in [k]$ and $t \in [T]$. We now form our VAR estimate for cluster ι :

$$\Gamma_\iota^{\text{VAR}} := \arg \min_{\Gamma \in \mathbf{R}^{m_\iota^2 d}} \left\{ \frac{1}{2T} \sum_{t=1}^T \|\widehat{\mathbf{y}}_\iota^{(t)} - (I_{m_\iota} \otimes (\widehat{\mathbf{x}}_\iota^{(t)})^\top) \Gamma\|_2^2 \right\}. \quad (5)$$

Theorem 2 (Recovery guarantee for mixed linear regression). *Suppose that Assumptions 1, 2, and 3 hold for the mixed linear regression problem. Additionally assume that the separation conditions of Corollary 1 hold. Then, with probability at least $1 - \delta - \exp(-0.08n)$, we have the following guarantee:*

$$\max_{\iota \in [k]} \|\Gamma_\iota^{\text{VAR}} - \Gamma_\iota^*\|_2 \leq \sqrt{2} \sqrt{\frac{\sigma^2 m^2 d}{T}} + \sqrt{3 \frac{\sigma^2}{T} \log \frac{k}{\delta}}.$$

This result is interesting because it indicates that, up to logarithmic and constant factors, the worst-case recovery error of Γ^* is $\sqrt{\frac{\sigma^2 m^2 d}{T}}$, which is the standard rate for a $(m^2 d)$ -dimensional parameter, with T samples and noise variance σ^2 .

5 Empirical Results

In this section we demonstrate the performance of our approach on both simulated and real-world datasets. Specifically, we show that our framework, in combination with a simple linear function class (AR/VAR), is able to outperform several recently proposed deep learning methods for time-series forecasting.

Setup. Given multivariate time series, we first use LinearSVR [18] for training local AR models. Then we use the learned AR coefficients to cluster the time series. To do so, we construct a K -nearest-neighbor graph ($K=11$) and then use the graph-clustering algorithm METIS [24] to form partitions. METIS is extremely scalable and has a sub-quadratic complexity in terms of the number of data points (n), unlike direct k -means or spectral clustering. Finally, we train global VAR models for each cluster using LinearSVR. We provide details about our implementation, including hyper-parameter settings, in the appendix in Section C. We refer to our algorithm as *Cluster & Conquer*.

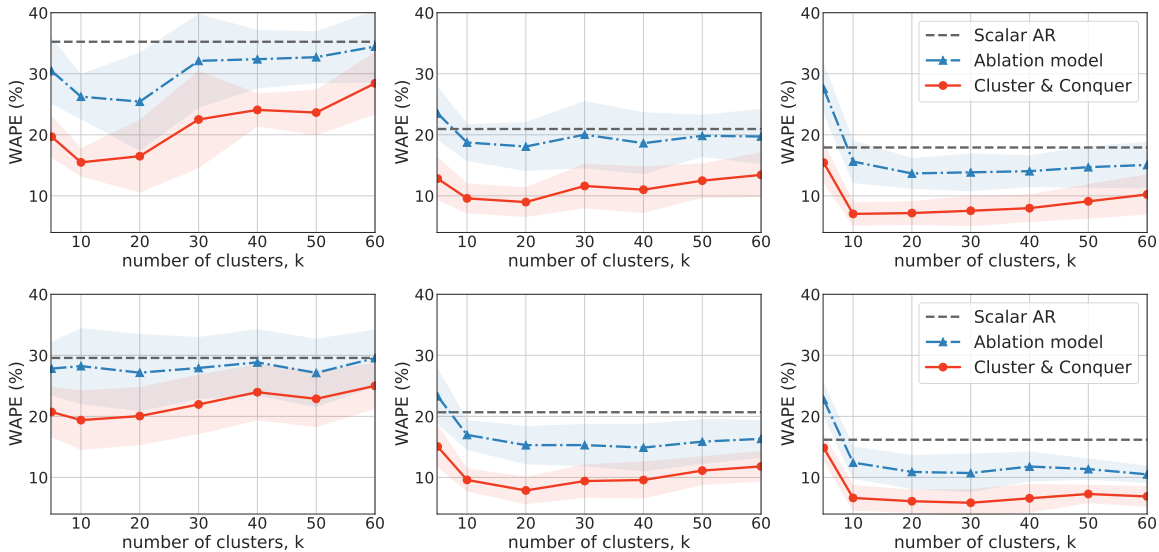


Figure 2: Here we demonstrate the performance of *Cluster & Conquer* on simulated data with different configurations. We evaluate our method as a function of the number of clusters and compare it to a Scalar AR model and an ablation model that uses random clusters. We see that *Cluster & Conquer* is always better than Scalar AR and the ablation model.

Experiments on simulated data. We perform a simulation study to empirically verify that our algorithm works for non-i.i.d time series data given our generative assumptions. To do so, we consider several different configurations, i.e., we vary the number of clusters and the lag and period of the ground truth time series data. In each case we construct dataset with $n = 200$ time series. Details about the data generation process are provided in the appendix in Section C.

Figure 2 shows results for the different configurations, along with 1-standard deviation bands over 20 runs. The top row shows results for data with period and lag of 20, whereas the bottom row shows results for data that have period and lag of 10. The three columns correspond to ground truth datasets that have 10, 20 and 30 clusters, respectively, from left to right.

To evaluate our model, we consider a rolling validation task with forecast horizon 24 and

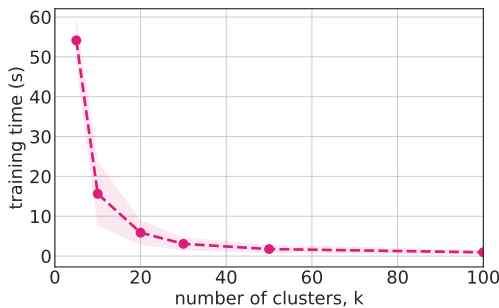


Figure 3: Training time of VAR models on the whole dataset decreases with an increase in number of clusters. When a cluster is too big, VAR cannot scale as the computation complexity increases super-quadratically w.r.t number of time series in the VAR model.

with 7 rolling windows. In each of the subplots, we plot the performance as measured by WAPE (see (15) in the appendix) as a function of the number of clusters (k) in our algorithm. We see that the performance of the algorithm is optimal or near-optimal at the correct value of k (i.e., when k is equal to number of clusters in the ground truth data). We also show that our method performs better compared to a Scalar AR model. Moreover, the performance is also better compared to an ablation model that considers random clusters followed by VAR within the clusters. We also note that the algorithm is robust to k provided k is not too far away from the number of clusters in the ground truth data.

In Figure 3, we plot the running time of the algorithm as k increases. As suspected when k is small the running time is prohibitive as the VAR model in each cluster has to learn $O((n/k)^2)$ parameters. The shaded area corresponds to the standard deviation across 20 runs.

| | MAE | RMSE | MAPE |
|------------------------------|-------------------|-------------------|-----------------|
| FC-LSTM [37] | 3.57 | 6.2 | 8.6 |
| SFM [44] | 2.75 | 4.32 | 6.6 |
| N-BEATS [33] | 3.41 | 5.52 | 7.65 |
| DCRNN [27] | 2.25 | 4.04 | 5.30 |
| LSTNet [26] | 2.34 | 4.26 | 5.41 |
| ST-GCN [41] | 2.25 | 4.04 | 5.26 |
| TCN [4] | 3.25 | 5.51 | 6.7 |
| DeepState [34] | 3.95 | 6.49 | 7.9 |
| DeepGLO [36] | 3.01 | 5.25 | 6.2 |
| StemGNN [9] | 2.14 | 4.01 | 5.01 |
| Scalar AR | 2.13±0.080 | 3.95±0.157 | 4.88±0.2 |
| <i>Cluster & Conquer</i> | 1.99±0.030 | 3.68±0.069 | 4.52±0.1 |

Table 1: Rolling validation results for the PEMS07 dataset.

| | MAE | RMSE | MAPE |
|------------------------------|--------------------|--------------------|-----------------|
| FC-LSTM [37] | 0.32 | 0.54 | 31.0 |
| SFM [44] | 0.17 | 0.58 | 11.9 |
| N-BEATS [33] | 0.08 | 0.16 | 12.428 |
| LSTNet [26] | 0.08 | 0.12 | 12.74 |
| TCN [4] | 0.1 | 0.3 | 19.03 |
| DeepState [34] | 0.09 | 0.76 | 19.21 |
| GraphWaveNet [40] | 0.19 | 0.86 | 19.67 |
| DeepGLO [36] | 0.09 | 0.15 | 12.45 |
| StemGNN [9] | 0.05 | 0.07 | 10.58 |
| Scalar AR | 0.024±0.000 | 0.041±0.000 | 5.67±0.1 |
| <i>Cluster & Conquer</i> | 0.023±0.000 | 0.040±0.001 | 5.39±0.0 |

Table 2: Rolling validation results for the ECG dataset.

Experiments on real data. Here, we follow the setups described by Cao et al. [9] and Sen et al. [36]. We refer the reader to the appendix, particularly Section C, for details about the baselines and our implementation, as well as statistics of the datasets. For all datasets, we choose the number of clusters in *Cluster & Conquer* to be $\lfloor n/10 \rfloor$, where n is the number

| | WAPE | MAPE | SMAPE |
|------------------------------|------------------|-------------------|------------------|
| DeepGLO [36] | 8.2 | 34.1 | 12.1 |
| TCN (LeveledInit) [36] | 9.2 | 23.7 | 12.6 |
| LSTM | 10.9 | 26.4 | 15.4 |
| DeepAR [35] | 8.6 | 25.9 | 14.1 |
| TCN [8] | 14.7 | 47.6 | 15.6 |
| Prophet [16] | 19.7 | 39.3 | 22.1 |
| TRMF [43] | 10.4 | 28.0 | 15.1 |
| SVD+TCN [36] | 21.9 | 43.7 | 23.8 |
| Scalar AR | 8.11±0.14 | 24.7±0.65 | 11.2±0.19 |
| <i>Cluster & Conquer</i> | 7.97±0.09 | 20.48±0.58 | 10.8±0.08 |

Table 3: Rolling val. results for the Electricity dataset.

| | WAPE | MAPE | SMAPE |
|------------------------------|------------------|-------------------|-------------|
| DeepGLO [36] | 14.8 | 16.8 | 14.2 |
| TCN (LeveledInit) [36] | 15.7 | 20.1 | 15.6 |
| LSTM | 27.0 | 35.7 | 26.3 |
| DeepAR [35] | 14.0 | 20.1 | 11.4 |
| TCN [8] | 20.4 | 28.4 | 23.6 |
| Prophet [16] | 30.3 | 55.9 | 42.0 |
| TRMF [43] | 15.9 | 22.6 | 18.1 |
| SVD+TCN [36] | 32.9 | 68.7 | 34.0 |
| Scalar AR | 15.9±0.31 | 20.0±1.14 | 15.72±0.74 |
| <i>Cluster & Conquer</i> | 14.0±0.16 | 17.18±0.49 | 13.68±0.33 |

Table 4: Rolling val. results for the Traffic dataset.

of time series. The number of clusters was manually tuned on the validation set between $\{\lfloor n/5 \rfloor, \lfloor n/10 \rfloor, \lfloor n/20 \rfloor\}$ and in all cases we found $\lfloor n/10 \rfloor$ to be the best.

First we compare the *Cluster & Conquer* approach to baselines reported by [9]. We show results for the PEMS07 [10] dataset in Table 1, and the ECG dataset [11] in Table 2. The *Cluster & Conquer* approach outperforms all other models on all metrics, including state-of-the-art deep learning models. This is remarkable, because we only instantiate our framework with linear models.

Next, we compare *Cluster & Conquer* against baselines reported by [36] for the Electricity and Traffic datasets, using the same metrics used in [36] for a fair comparison. Table 3 shows results for the Electricity dataset. Here, the advantage of the *Cluster & Conquer* approach is pronounced, i.e., the gap between our approach and other deep learning models is distinct on all three metrics. On the other hand, the performance gap is less distinct for the Traffic dataset in Table 4.

Given these results, a few remarks are in place. First, it should be noted that the *Cluster & Conquer* approach always improves over the scalar AR model. This shows that capturing intra-cluster dependencies is important for forecasting. Second, the *Cluster & Conquer* approach is competitive to global deep learning models (e.g. DeepGLO, DCRNN, LSTNet). One reason for that is that the *Cluster & Conquer* approach suppresses noise from irrelevant time series when predicting the future of a particular time series. Third, the *Cluster & Conquer* approach does not use specially designed covariates. For instance, DeepAR [35] uses specially designed

time-based covariates such as transformations of days of the week, and holidays.

6 Conclusions

We proposed a three-stage framework, based on a divide and conquer principle, for large-scale multivariate time-series forecasting. Our *Cluster & Conquer* framework is highly flexible, i.e., it allows for the use of any multivariate time-series model coupled with a scalable clustering algorithm. In turn, this framework is computationally efficient, embarrassingly parallel, and typically more efficient than dense vector auto regression. We provide theoretical guarantees for our framework in a mixed linear regression setting. Experiments on both synthetic and multiple real-world datasets show that the *Cluster & Conquer* approach achieves state-of-the-art results compared to baselines.

References

- [1] S. Aghabozorgi, A. Seyed Shirخورshidi, and T. Ying Wah. Time-series clustering - a decade review. *Inf. Syst.*, 53(C):16–38, Oct. 2015. ISSN 0306-4379. doi: 10.1016/j.is.2015.04.007. URL <https://doi.org/10.1016/j.is.2015.04.007>.
- [2] O. Azencot, N. B. Erichson, V. Lin, and M. Mahoney. Forecasting sequential data using consistent koopman autoencoders. In *International Conference on Machine Learning*, pages 475–485. PMLR, 2020.
- [3] L. Bai, L. Yao, C. Li, X. Wang, and C. Wang. Adaptive graph convolutional recurrent network for traffic forecasting. *Advances in Neural Information Processing Systems*, 33, 2020.
- [4] S. Bai, J. Z. Kolter, and V. Koltun. An empirical evaluation of generic convolutional and recurrent networks for sequence modeling. *CoRR*, abs/1803.01271, 2018. URL <http://arxiv.org/abs/1803.01271>.
- [5] K. Bandara, C. Bergmeir, and S. Smyl. Forecasting across time series databases using recurrent neural networks on groups of similar series: A clustering approach. *Expert Syst. Appl.*, 140, 2020. doi: 10.1016/j.eswa.2019.112896. URL <https://doi.org/10.1016/j.eswa.2019.112896>.
- [6] K. Benidis, S. S. Rangapuram, V. Flunkert, B. Wang, D. Maddix, C. Turkmen, J. Gasthaus, M. Bohlke-Schneider, D. Salinas, L. Stella, et al. Neural forecasting: Introduction and literature overview. *arXiv preprint arXiv:2004.10240*, 2020.
- [7] N. Bhatia et al. Survey of nearest neighbor techniques. *arXiv preprint arXiv:1007.0085*, 2010.
- [8] A. Borovykh, S. Bohte, and C. W. Oosterlee. Conditional time series forecasting with convolutional neural networks. *arXiv preprint arXiv:1703.04691*, 2017.
- [9] D. Cao, Y. Wang, J. Duan, C. Zhang, X. Zhu, C. Huang, Y. Tong, B. Xu, J. Bai, J. Tong, and Q. Zhang. Spectral temporal graph neural network for multivariate

- time-series forecasting. In H. Larochelle, M. Ranzato, R. Hadsell, M. Balcan, and H. Lin, editors, *Advances in Neural Information Processing Systems 33: Annual Conference on Neural Information Processing Systems 2020, NeurIPS 2020, December 6-12, 2020, virtual*, 2020. URL <https://proceedings.neurips.cc/paper/2020/hash/cdf6581cb7aca4b7e19ef136c6e601a5-Abstract.html>.
- [10] C. Chen, K. Petty, A. Skabardonis, P. Varaiya, and Z. Jia. Freeway performance measurement system: Mining loop detector data. *Transportation Research Record*, 1748(1):96–102, 2001. doi: 10.3141/1748-12. URL <https://doi.org/10.3141/1748-12>.
- [11] H. A. Dau, A. J. Bagnall, K. Kamgar, C. M. Yeh, Y. Zhu, S. Gharghabi, C. A. Ratanamahatana, and E. J. Keogh. The UCR time series archive. *IEEE CAA J. Autom. Sinica*, 6(6):1293–1305, 2019. doi: 10.1109/jas.2019.1911747. URL <https://doi.org/10.1109/jas.2019.1911747>.
- [12] R. Ding, Q. Wang, Y. Dang, Q. Fu, H. Zhang, and D. Zhang. Yading: fast clustering of large-scale time series data. *Proceedings of the VLDB Endowment*, 8(5):473–484, 2015.
- [13] D. V. Divine. M. mudelsee, , climate time series analysis: Classical statistical and bootstrap methods (2010) springer, dordrecht 978-90-481-9482-7. *Comput. Geosci.*, 43:24, 2012. doi: 10.1016/j.cageo.2012.02.030. URL <https://doi.org/10.1016/j.cageo.2012.02.030>.
- [14] N. B. Erichson, M. Muehlebach, and M. W. Mahoney. Physics-informed autoencoders for lyapunov-stable fluid flow prediction. *arXiv preprint arXiv:1905.10866*, 2019.
- [15] N. B. Erichson, O. Azencot, A. Queiruga, L. Hodgkinson, and M. W. Mahoney. Lipschitz recurrent neural networks. In *International Conference on Learning Representations*, 2021. URL <https://openreview.net/forum?id=-N7PBXqOUJZ>.
- [16] Facebook. Fb prophet, forecasting at scale. <https://github.com/facebook/prophet>, 2020.
- [17] C. Faloutsos, V. Flunkert, J. Gasthaus, T. Januschowski, and Y. Wang. Forecasting big time series: Theory and practice. In A. E. F. Seghrouchni, G. Sukthankar, T. Liu, and M. van Steen, editors, *Companion of The 2020 Web Conference 2020, Taipei, Taiwan, April 20-24, 2020*, pages 320–321. ACM / IW3C2, 2020. doi: 10.1145/3366424.3383118. URL <https://doi.org/10.1145/3366424.3383118>.
- [18] R. Fan, K. Chang, C. Hsieh, X. Wang, and C. Lin. LIBLINEAR: A library for large linear classification. *J. Mach. Learn. Res.*, 9:1871–1874, 2008. URL <https://dl.acm.org/citation.cfm?id=1442794>.
- [19] A. Goldenshluger and A. Zeevi. Nonasymptotic bounds for autoregressive time series modeling. *Ann. Statist.*, 29(2):417–444, 2001. ISSN 0090-5364. doi: 10.1214/aos/1009210547. URL <https://doi.org/10.1214/aos/1009210547>.
- [20] S. Guo, Y. Wang, and Q. Yao. High-dimensional and banded vector autoregressions. *Biometrika*, 103(4):889–903, 2016. ISSN 0006-3444. doi: 10.1093/biomet/asw046. URL <https://doi.org/10.1093/biomet/asw046>.
- [21] R. J. Hyndman and G. Athanasopoulos. *Forecasting: principles and practice*. OTexts, 2018.

- [22] K. Kalpakis, D. Gada, and V. Puttagunta. Distance measures for effective clustering of ARIMA time-series. In N. Cercone, T. Y. Lin, and X. Wu, editors, *Proceedings of the 2001 IEEE International Conference on Data Mining, 29 November - 2 December 2001, San Jose, California, USA*, pages 273–280. IEEE Computer Society, 2001. doi: 10.1109/ICDM.2001.989529. URL <https://doi.org/10.1109/ICDM.2001.989529>.
- [23] R. Kannan and S. Vempala. Spectral algorithms. *Found. Trends Theor. Comput. Sci.*, 4(3-4):front matter, 157–288 (2009), 2008. ISSN 1551-305X. doi: 10.1561/0400000025. URL <https://doi.org/10.1561/0400000025>.
- [24] G. Karypis and V. Kumar. *MeTiS: A Software Package for Partitioning Unstructured Graphs, Partitioning Meshes, and Computing Fill-Reducing Orderings of Sparse Matrices*. Department of Computer Science, University of Minnesota, version 4.0 edition, Sept. 1998.
- [25] V. Kuznetsov and M. Mohri. Learning theory and algorithms for forecasting non-stationary time series. In *NIPS*, pages 541–549. Citeseer, 2015.
- [26] G. Lai, W. Chang, Y. Yang, and H. Liu. Modeling long- and short-term temporal patterns with deep neural networks. In K. Collins-Thompson, Q. Mei, B. D. Davison, Y. Liu, and E. Yilmaz, editors, *The 41st International ACM SIGIR Conference on Research & Development in Information Retrieval, SIGIR 2018, Ann Arbor, MI, USA, July 08-12, 2018*, pages 95–104. ACM, 2018. doi: 10.1145/3209978.3210006. URL <https://doi.org/10.1145/3209978.3210006>.
- [27] Y. Li, R. Yu, C. Shahabi, and Y. Liu. Diffusion convolutional recurrent neural network: Data-driven traffic forecasting. *arXiv preprint arXiv:1707.01926*, 2017.
- [28] Y. Li, R. Yu, C. Shahabi, and Y. Liu. Diffusion convolutional recurrent neural network: Data-driven traffic forecasting. In *International Conference on Learning Representations*, 2018.
- [29] S. H. Lim, N. B. Erichson, L. Hodgkinson, and M. W. Mahoney. Noisy recurrent neural networks. *arXiv preprint arXiv:2102.04877*, 2021.
- [30] M. Löffler, A. Y. Zhang, and H. H. Zhou. Optimality of spectral clustering for gaussian mixture model. *CoRR*, abs/1911.00538, 2019. URL <http://arxiv.org/abs/1911.00538>.
- [31] Y. Matsubara, Y. Sakurai, W. G. van Panhuis, and C. Faloutsos. FUNNEL: automatic mining of spatially coevolving epidemics. In S. A. Macskassy, C. Perlich, J. Leskovec, W. Wang, and R. Ghani, editors, *The 20th ACM SIGKDD International Conference on Knowledge Discovery and Data Mining, KDD '14, New York, NY, USA - August 24 - 27, 2014*, pages 105–114. ACM, 2014. doi: 10.1145/2623330.2623624. URL <https://doi.org/10.1145/2623330.2623624>.
- [32] D. J. McDonald, C. R. Shalizi, and M. Schervish. Nonparametric risk bounds for time-series forecasting. *J. Mach. Learn. Res.*, 18:Paper No. 32, 40, 2017. ISSN 1532-4435.
- [33] B. N. Oreshkin, D. Carpov, N. Chapados, and Y. Bengio. N-BEATS: neural basis expansion analysis for interpretable time series forecasting. In *8th International Conference on Learning Representations, ICLR 2020, Addis Ababa, Ethiopia, April 26-30, 2020*. OpenReview.net, 2020. URL <https://openreview.net/forum?id=r1ecqn4YwB>.

- [34] S. S. Rangapuram, M. W. Seeger, J. Gasthaus, L. Stella, Y. Wang, and T. Januschowski. Deep state space models for time series forecasting. In S. Bengio, H. M. Wallach, H. Larochelle, K. Grauman, N. Cesa-Bianchi, and R. Garnett, editors, *Advances in Neural Information Processing Systems 31: Annual Conference on Neural Information Processing Systems 2018, NeurIPS 2018, December 3-8, 2018, Montréal, Canada*, pages 7796–7805, 2018. URL <https://proceedings.neurips.cc/paper/2018/hash/5cf68969fb67aa6082363a6d4e6468e2-Abstract.html>.
- [35] D. Salinas, V. Flunkert, J. Gasthaus, and T. Januschowski. Deepar: Probabilistic forecasting with autoregressive recurrent networks. *International Journal of Forecasting*, 2019.
- [36] R. Sen, H. Yu, and I. S. Dhillon. Think globally, act locally: A deep neural network approach to high-dimensional time series forecasting. In H. M. Wallach, H. Larochelle, A. Beygelzimer, F. d’Alché-Buc, E. B. Fox, and R. Garnett, editors, *Advances in Neural Information Processing Systems 32: Annual Conference on Neural Information Processing Systems 2019, NeurIPS 2019, December 8-14, 2019, Vancouver, BC, Canada*, pages 4838–4847, 2019. URL <https://proceedings.neurips.cc/paper/2019/hash/3a0844cee4fcf57de0c71e9ad3035478-Abstract.html>.
- [37] I. Sutskever, O. Vinyals, and Q. V. Le. Sequence to sequence learning with neural networks. In Z. Ghahramani, M. Welling, C. Cortes, N. D. Lawrence, and K. Q. Weinberger, editors, *Advances in Neural Information Processing Systems 27: Annual Conference on Neural Information Processing Systems 2014, December 8-13 2014, Montreal, Quebec, Canada*, pages 3104–3112, 2014. URL <https://proceedings.neurips.cc/paper/2014/hash/a14ac55a4f27472c5d894ec1c3c743d2-Abstract.html>.
- [38] B. Venkataramana Kini and C. Chandra Sekhar. Bayesian mixture of AR models for time series clustering. *PAA Pattern Anal. Appl.*, 16(2):179–200, 2013. ISSN 1433-7541. doi: 10.1007/s10044-011-0247-5. URL <https://doi.org/10.1007/s10044-011-0247-5>.
- [39] T. Warren Liao. Clustering of time series data—a survey. *Pattern Recogn.*, 38(11):1857–1874, Nov. 2005. ISSN 0031-3203. doi: 10.1016/j.patcog.2005.01.025. URL <https://doi.org/10.1016/j.patcog.2005.01.025>.
- [40] Z. Wu, S. Pan, G. Long, J. Jiang, and C. Zhang. Graph wavenet for deep spatial-temporal graph modeling. In *IJCAI*, 2019.
- [41] B. Yu, H. Yin, and Z. Zhu. Spatio-temporal graph convolutional networks: A deep learning framework for traffic forecasting. *arXiv preprint arXiv:1709.04875*, 2017.
- [42] B. Yu, H. Yin, and Z. Zhu. Spatio-temporal graph convolutional networks: a deep learning framework for traffic forecasting. In *Proceedings of the 27th International Joint Conference on Artificial Intelligence*, pages 3634–3640, 2018.
- [43] H.-F. Yu, N. Rao, and I. S. Dhillon. Temporal regularized matrix factorization for high-dimensional time series prediction. In *Advances in neural information processing systems*, pages 847–855, 2016.
- [44] L. Zhang, C. C. Aggarwal, and G. Qi. Stock price prediction via discovering multi-frequency trading patterns. In *Proceedings of the 23rd ACM SIGKDD International*

Conference on Knowledge Discovery and Data Mining, Halifax, NS, Canada, August 13 - 17, 2017, pages 2141–2149. ACM, 2017. doi: 10.1145/3097983.3098117. URL <https://doi.org/10.1145/3097983.3098117>.

- [45] Y. Zhu and D. E. Shasha. Statstream: Statistical monitoring of thousands of data streams in real time. In *Proceedings of 28th International Conference on Very Large Data Bases, VLDB 2002, Hong Kong, August 20-23, 2002*, pages 358–369. Morgan Kaufmann, 2002. doi: 10.1016/B978-155860869-6/50039-1. URL <http://www.vldb.org/conf/2002/S10P04.pdf>.

A Proof of result for near mixture of Gaussians

Notation: Let us define the following loss function, $\ell: [k]^{[n]} \times [k]^{[n]} \rightarrow \mathbf{R}_+$, given by

$$\ell(\mathbf{c}, \mathbf{c}') := \min_{\varphi} \sum_{i=1}^n \mathbf{1}\left\{c(i) \neq \varphi(c'(i))\right\}, \quad \text{for any } \mathbf{c}, \mathbf{c}' \in [k]^{[n]},$$

where the minimum ranges over bijections $\varphi: [k] \rightarrow [k]$. Intuitively, this measures the number disagreements between the cluster labellings \mathbf{c}, \mathbf{c}' . Let us set

$$\Delta := \min_{i \neq j \in [k]} \|\theta_i^* - \theta_j^*\|_2$$

Proof: Since Algorithms 2 and 3 differ only by the application of the orthogonal matrix \widehat{U} , it is straightforward to see that there is a bijection $\phi: [k] \rightarrow [k]$ such that $\widehat{\mathbf{c}}_{\text{appx}}(i) = \phi(\widehat{\mathbf{c}}_{\text{spec}}(i))$ for each $i \in [n]$. Therefore, by definition of $\ell(\cdot, \cdot)$, we have that

$$\ell(\widehat{\mathbf{c}}_{\text{spec}}, \mathbf{c}^*) = \ell(\widehat{\mathbf{c}}_{\text{appx}}, \mathbf{c}^*).$$

Suppose that the following good event holds:

$$\mathcal{E} := \left\{ \|G\|_{\text{op}} \leq \sqrt{2\gamma}(\sqrt{n} + \sqrt{d}) \right\}.$$

Consider the sets

$$\mathcal{I}_{\text{bad}} := \left\{ i \in [n] : \|\theta_{\mathbf{c}^*(i)}^* - \widehat{\theta}_i\|_2 \geq \Delta/2 \right\} \quad \text{and} \quad \mathcal{I}_{\text{good}} := [n] \setminus \mathcal{I}_{\text{bad}}.$$

Under \mathcal{E} , it is possible to show that

$$|\mathcal{I}_{\text{bad}}| \leq \frac{128k \|G\|_{\text{op}}^2}{\Delta^2} \leq \frac{512\gamma k(n+d)}{\Delta^2}.$$

(The first inequality above is Proposition 1.) We can partition the good indices into disjoint sets I_j as follows:

$$I_j := \left\{ i \in [n] : \mathbf{c}^*(i) = j, \|\widehat{\theta}_i - \theta_{\mathbf{c}^*(i)}^*\|_2 < \Delta/2 \right\}, \quad j = 1, \dots, k.$$

Note that under the assumption on Δ , $|\mathcal{I}_{\text{bad}}| \leq \frac{\beta n}{2k}$, which implies that I_j are nonempty for all $j \in [k]$. Additionally, $\widehat{\mathbf{c}}_{\text{appx}}(I_j)$ are pairwise disjoint, as we demonstrate in Lemma 4, after which it follows that there exists a permutation φ such that

$$\varphi(\widehat{\mathbf{c}}_{\text{appx}}(i)) = j, \quad \text{for each } i \in I_j.$$

This implies that under \mathcal{E}

$$\ell(\widehat{\mathbf{c}}_{\text{appx}}, \mathbf{c}^*) \leq |\mathcal{I}_{\text{bad}}| \leq \frac{512\gamma k(n+d)}{\Delta^2} \leq \frac{1}{2},$$

which implies that $\widehat{\mathbf{c}}_{\text{appx}}, \mathbf{c}^*$ are equal up to permutation. The result now follows by noting that $\mathbf{P}(\mathcal{E}) \geq 1 - e^{-0.08n}$, as we show in Lemma 3.

A.1 Auxillary results for Theorem 1

We assume that for all i , we have $\Sigma_i \preceq \gamma I_d$ for some constant $\gamma > 0$. It will be convenient for us to consider the sample matrix $X \in \mathbf{R}^{d \times n}$, which has columns $X_1, \dots, X_n \in \mathbf{R}^d$. Then it is easy to see that

$$X = \mathbf{E}X + (X - \mathbf{E}X) =: \Theta^* + G,$$

where $\Theta^*, G \in \mathbf{R}^{d \times n}$. In the decomposition above, Θ^* has columns $\theta_{c^*(1)}^*, \dots, \theta_{c^*(n)}^*$, whereas G has columns $g_1, \dots, g_n \in \mathbf{R}^d$, where

$$g_i \stackrel{\text{ind.}}{\sim} \mathbf{N}(0, \Sigma_i), \quad i = 1, \dots, n.$$

Lemma 3. *Let $Z \in \mathbf{R}^{d \times n}$ be a random matrix with columns $z_i \stackrel{\text{ind.}}{\sim} \mathbf{N}(0, \Sigma_i)$, for $i = 1, \dots, n$. Let $\lambda_{\max} := \max_{i=1, \dots, n} \left\| \Sigma_i^{1/2} \right\|_{\text{op}}$. Then*

$$\mathbf{P} \left\{ \|Z\|_{\text{op}} \geq \lambda_{\max}(\sqrt{n} + \sqrt{d} + t) \right\} \leq \exp\left(-\frac{t^2}{2}\right).$$

Proof. We note that $\|Z\|_{\text{op}} \leq \lambda_{\max} \|W\|_{\text{op}}$ almost surely since we can write the columns of Z as $z_i = \Sigma_i^{1/2} w_i$ in distribution, where $w_i \stackrel{\text{ind.}}{\sim} \mathbf{N}(0, I_d)$. Consequently,

$$\mathbf{P} \left\{ \|Z\|_{\text{op}} \geq \lambda_{\max}(\sqrt{n} + \sqrt{d} + t) \right\} \leq \mathbf{P} \left\{ \|W\|_{\text{op}} \leq \sqrt{n} + \sqrt{d} + t \right\} \leq e^{-t^2/2},$$

by standard concentration bounds for Gaussian random matrices. \square

We record the following corollary. To do so, we first consider the following ‘good’ event, when the operator norm of the noise matrix G is small enough.

$$\mathcal{E} := \left\{ \|G\|_{\text{op}} \leq \sqrt{2\gamma}(\sqrt{n} + \sqrt{d}) \right\} \quad (6)$$

Corollary 2. *We have $\mathbf{P}(\mathcal{E}) \geq 1 - e^{-0.08n}$.*

Proof. In Lemma 3, we may set $Z = G$, and take $\lambda_{\max} := \sqrt{\gamma}$. The result follows by taking $t = (\sqrt{2} - 1)(\sqrt{d} + \sqrt{n}) \geq \sqrt{0.4n}$. \square

To finish the proof, we first introduce an alternative algorithm which is simpler to analyze, which we refer to in the sequel as Algorithm (3).

Algorithm 3 [Clustering via low-rank approximation] *Algorithm for estimating clusters from samples.*

input: sample matrix $X \in \mathbf{R}^{d \times n}$, number of clusters, k

1. Compute truncated singular value decomposition of sample matrix.

$$X_k := \sum_{i=1}^k \hat{\sigma}_i \hat{u}_i \hat{v}_i^\top =: \hat{U} \hat{\Sigma} \hat{V}^\top \in \mathbf{R}^{d \times n}$$

2. Solve k -means on the columns of Y . Compute a solution to the optimization problem

$$\text{minimize} \quad \frac{1}{2n} \sum_{i=1}^n \|X_i - \theta_{\kappa_i}\|_2^2,$$

with variables $\theta_1, \dots, \theta_k \in \mathbf{R}^d$ and $\kappa_1, \dots, \kappa_n \in [k]$.

output: estimates for labelling $\hat{c}_{\text{appx}}(\cdot): [n] \rightarrow [k]$, where $\hat{c}_{\text{appx}}(i) := \kappa_i^*$, for all i .

It turns out that there is a bijection $\phi: [k] \rightarrow [k]$ such that $\widehat{\mathbf{c}}_{\text{appx}}(i) = \phi(\widehat{\mathbf{c}}_{\text{spec}}(i))$ for each $i \in [n]$ (for additional details, see Lemma 4.1 of [30]). Therefore, by definition of $\ell(\cdot, \cdot)$, we have that

$$\ell(\widehat{\mathbf{c}}_{\text{spec}}, \mathbf{c}^*) = \ell(\widehat{\mathbf{c}}_{\text{appx}}, \mathbf{c}^*),$$

and so it suffices to analyze the output of the algorithm that simply uses the rank- k approximant to X , algorithm 3.

To do so, let us first introduce the following two sets of indices:

$$\mathcal{I}_{\text{bad}} := \left\{ i \in [n] : \|\theta_{\mathbf{c}^*(i)}^* - \widehat{\theta}_i\|_2 \geq \Delta/2 \right\} \quad \text{and} \quad \mathcal{I}_{\text{good}} := [n] \setminus \mathcal{I}_{\text{bad}}.$$

Above, $\widehat{\theta}_i$ is the optimal solution θ_i^* in step 2 of Algorithm 3. We will also use the notation $\widehat{\Theta} \in \mathbf{R}^{d \times n}$ to denote the matrix which has columns $\widehat{\theta}_i$. Note that $\widehat{\Theta}$ by construction is the projection of the rank- k approximant X_k onto the set of matrices with at most k distinct columns, in the Frobenius norm.

We then have the following proposition.

Proposition 1. *The cardinality of the set of bad indices enjoys the following upper bound:*

$$|\mathcal{I}_{\text{bad}}| \leq \frac{128k \|G\|_{\text{op}}^2}{\Delta^2},$$

almost surely.

Proof. Note that

$$\left\| \widehat{\Theta} - \Theta^* \right\|_{\text{F}}^2 = \sum_{i=1}^n \|\theta_{\mathbf{c}^*(i)}^* - \widehat{\theta}_i\|_2^2 \geq |\mathcal{I}_{\text{bad}}| \frac{\Delta^2}{4}.$$

Therefore, we see that

$$|\mathcal{I}_{\text{bad}}| \leq \frac{4}{\Delta^2} \left\| \widehat{\Theta} - \Theta^* \right\|_{\text{F}}^2 \tag{7}$$

Note that since $\widehat{\Theta}, \Theta^*$ are both (at most) rank- k matrices we evidently have

$$\left\| \widehat{\Theta} - \Theta^* \right\|_{\text{F}} \leq \sqrt{2k} \left\| \widehat{\Theta} - \Theta^* \right\|_{\text{op}} \leq \sqrt{8k} \|\Theta^* - X_k\|_{\text{op}},$$

where in the last inequality we use the optimality of $\widehat{\Theta}$ along with the triangle inequality. Adding and subtracting X , and then relying on Eckart-Young, the display above implies

$$\left\| \widehat{\Theta} - \Theta^* \right\|_{\text{F}} \leq \sqrt{32k} \|X - \Theta^*\|_{\text{op}} \leq \|G\|_{\text{op}} \sqrt{32k}.$$

Applying the display above in the cardinality bound (7) gives the result. \square

Additionally, we define the following sets

$$I_j := \left\{ i \in [n] : \mathbf{c}^*(i) = j, \|\widehat{\theta}_i - \theta_{\mathbf{c}^*(i)}^*\|_2 < \Delta/2 \right\}, \quad j = 1, \dots, k.$$

Clearly, we have that $\{I_j\}$ form a disjoint partition of $\mathcal{I}_{\text{good}}$. However, as the following result shows, these sets are also pairwise disjoint and nonempty under the estimated clustering, $\widehat{\mathbf{c}}_{\text{appx}}(\cdot)$.

Lemma 4. *The sets $\widehat{c}_{\text{appx}}(I_j)$ are disjoint for each $j \in [k]$.*

Proof. By contradiction, suppose that $\widehat{c}_{\text{appx}}(I_{j_1}) \cap \widehat{c}_{\text{appx}}(I_{j_2}) \neq \emptyset$, for some $j_1 \neq j_2 \in [k]$. This happens if and only if there exists $i_1, i_2 \in \mathcal{I}_{\text{good}}$ and $j_0 \in [k]$ for which:

$$c^*(i_1) = j_1, \quad c^*(i_2) = j_2, \quad \text{and} \quad j_0 = \widehat{c}_{\text{appx}}(i_1) = \widehat{c}_{\text{appx}}(i_2). \quad (8)$$

However, then we note that

$$\begin{aligned} \|\theta_{j_1}^* - \theta_{j_2}^*\|_2 &\leq \|\theta_{c^*(i_1)}^* - \widehat{\theta}_{\widehat{c}_{\text{appx}}(i_1)}\|_2 + \|\widehat{\theta}_{\widehat{c}_{\text{appx}}(i_1)} - \widehat{\theta}_{\widehat{c}_{\text{appx}}(i_2)}\|_2 + \|\widehat{\theta}_{\widehat{c}_{\text{appx}}(i_2)} - \theta_{c^*(i_2)}^*\|_2 \\ &\quad \text{(by triangle inequality, conditions (8))} \\ &= \|\theta_{c^*(i_1)}^* - \widehat{\theta}_{j_0}\|_2 + \|\widehat{\theta}_{j_0} - \theta_{c^*(i_2)}^*\|_2 \quad \text{(since } j_0 = \widehat{c}_{\text{appx}}(i_1) = \widehat{c}_{\text{appx}}(i_2)\text{)} \\ &< \Delta, \quad \text{(since } i_1, i_2 \in \mathcal{I}_{\text{good}}\text{)} \end{aligned}$$

which contradicts the definition of Δ . \square

B Other deferred proofs

Proof of Lemma 1. Following the normal equations for the scalar autoregression problem (2),

$$\widehat{\theta}_i^{\text{AR}} = \theta_i + \widehat{\Sigma}_i^{-1} \left\{ \frac{1}{T} \sum_{t=1}^T \Upsilon(\varepsilon_i^{(t)} + \Delta_i^{(t)}) x_i^{(t)} \right\}. \quad (9)$$

Above we defined $\Delta_i^{(t)} := \sum_{j:c_j=c_i} \gamma_{ij}^\top x_j^{(t)}$. Note that

$$\Delta_i^{(t)} \stackrel{d}{=} \mathbf{N}\left(0, (\tau \rho_i^{(t)})^2\right), \quad \text{where} \quad \rho_i^{(t)} := \left(\sum_{j:c_j=c_i} \|x_j^{(t)}\|_2^2 \right)^{\frac{1}{2}}.$$

Therefore in view of (9), we see that $\widehat{\theta}_i^{\text{AR}}$ is indeed a sum of Gaussians with mean $\bar{\theta}_{c_i}$ and covariance

$$\Lambda_i = \nu^2 I_d + \frac{\sigma^2}{T} \widehat{\Sigma}_i^{-1} + \frac{\sigma^2}{T} \widehat{\Sigma}_i^{-2} \widehat{\Sigma}_i(\rho_i),$$

which proves the result. \square

Proof of Lemma 2. To lighten notation, we define

$$Z_t := I_m \otimes (x^{(t)})^\top, \quad t \in [T].$$

Note that $Z_t \in \mathbf{R}^{m \times m^2 d}$. It follows from the optimality condition for the VAR problem that we have the following decomposition:

$$\Gamma^{\text{VAR}} = \left(\frac{1}{T} \sum_{t=1}^T Z_t^\top Z_t \right)^{-1} \frac{1}{T} \sum_{t=1}^T Z_t^\top \varepsilon^{(t)} = \Gamma^* + \frac{1}{T} \sum_{t=1}^T Z_t^\top \varepsilon^{(t)},$$

where above we use the isotropy assumption. The decomposition above then immediately implies that

$$\Gamma^{\text{VAR}} \sim \mathbf{N}\left(\Gamma^*, \frac{\sigma^2}{T} I_{m^2 d}\right).$$

Note that $\frac{T}{\sigma^2} \|(\Gamma^{\text{VAR}} - \Gamma^*)\|_2^2$ is equal in distribution to a χ^2 random variable with $m^2 d$ -degrees of freedom. The result now follows by using standard concentration bounds for χ^2 -random variables. \square

C Implementation Details

Simulation Study. In the simulation experiment in Figure 2, we generate a synthetic dataset, where there are n time series grouped into k clusters of equal size. In cluster i , the local AR parameters for every time series is centered at $\theta_{c(i)} = z_i/C_i$ where z_i is generated from $\mathbf{N}(0, I_d)$ distribution and C_i is a constant. The noise around $\theta_{c(i)}$ is set to have a standard deviation of $1e-2$. The VAR parameters for time series in a cluster is also generated from the standard normal distribution. In other words $\gamma_{i,j} = z_{ij}/C_{ij}$ where $z_{ij} \sim \mathbf{N}(0, I_d)$ if $c(i) = c(j)$. The constants C_i 's and C_{ij} 's are chosen such that the ℓ_p norm of all the lag coefficients of any particular time series is one for $p = 2.5$. The choice of the normalization is made to promote stationarity. We also restrict the values of the time series between $[-1, 1]$. Thus the time-series progression is governed by the equation,

$$y_i^{(t)} = \min \left(1, \max \left(\theta_i^\top y_i^{(t-d:t-1)} + \sum_{j:c(i)=c(j)} \gamma_{ij}^\top y_j^{(t-d:t-1)} + \varepsilon_i^{(t)}, -1 \right) \right). \quad (10)$$

Learning Algorithm. The scalar AR algorithm is implemented using one LinearSVR [18] instance per time series. Similarly the VAR models are also implemented using one LinearSVR instance per cluster. We tune the parameters of the AR model on a randomly chosen time series from the whole datasets and then held fixed for all other time series. The hyper-parameters are tuned via grid-search among the grid `{"max_iter": [1000], "C": np.logspace(-4, 0, 10), "epsilon": [0, 1e-1, 1e-2, 1e-3]}`. Similarly the VAR hyper-parameters are tuned on a randomly chosen cluster among the same grid parameters as above, and then held fixed.

Lag Indices. These are very important parameters for both the AR and VAR model. For hourly datasets like Electricity and Traffic, we use the lag indices `np.concatenate([np.arange(1, 25), np.arange(7*24, 8*24), np.arange(14*24, 15*24)])` i.e the last 24 hours, 24 hours on the same day last week and 24 hrs on the same day two weeks back. For the datasets in 5min intervals, like ECG and PEMS07 we set the lag indices as `np.concatenate([np.arange(1, 12), np.arange(12, 15), np.arange(24, 27)])` i.e the last hour, the corresponding 15 min in the last hour and the corresponding 15 minutes two hours back.

Clustering. We cluster on the learnt AR parameters normalized to ℓ_2 norm one. We fit a KD-Tree [7] in the AR parameter set and form a K -nn graph using 11 neighbors for each point. Then we use METIS graph clustering on this graph. In general we set the number of clusters to be $k = \lfloor n/10 \rfloor$ for a dataset with n time series. We tuned the k among $\{\lfloor n/5 \rfloor, \lfloor n/10 \rfloor, \lfloor n/20 \rfloor\}$, and $k = \lfloor n/10 \rfloor$ was close to optimal among the three on all 4 datasets.

Baselines. Now we can present details about the baselines. For the first two experiments i.e the ones on ECG and PEMS07 all the baselines are in a setting identical to the ones used in [9]. We merely recreate the values from the table in [9]. It is a fair comparison as our algorithms are also evaluated on the exact same task. Similarly for the experiments on Traffic and Electricity dataset the baseline numbers are taken from Table 2 in [36]. We make these choices for the ease of reproducibility, moving forward.

| Dataset | Num. Series (n) | Num. Training Points (t) | Forecast Horizon (τ) | Rolling Windows (n_w) | Granularity |
|-------------|---------------------|------------------------------|-----------------------------|---------------------------|-------------|
| Electricity | 370 | 25,968 | 24 | 7 | Hourly |
| Traffic | 963 | 10,392 | 24 | 7 | Hourly |
| PEMS07 | 208 | 11,232 | 3 | 480 | 5min |
| ECG | 140 | 4,999 | 3 | 167 | 5min |

Table 5: We present the salient features of the datasets. We use the last $n_w \times \tau$ time-points to construct the test sets. Then, we perform rolling validation with a forecast horizon of τ and number of rolling windows as n_w .

D Metrics

The following well-known loss metrics are used in this paper. Here, $\mathbf{Y} \in \mathbf{R}^{n' \times t'}$ represents the actual values while $\hat{\mathbf{Y}} \in \mathbf{R}^{n' \times t'}$ are the corresponding predictions.

(i) **WAPE:** Weighted Absolute Percent Error is defined as follows,

$$\mathcal{L}_w(\hat{\mathbf{Y}}, \mathbf{Y}) = \frac{\sum_{i=1}^{n'} \sum_{j=1}^{t'} |Y_{ij} - \hat{Y}_{ij}|}{\sum_{i=1}^{n'} \sum_{j=1}^{t'} |Y_{ij}|}. \quad (11)$$

(ii) **MAPE:** Mean Absolute Percent Error is defined as follows,

$$\mathcal{L}_m(\hat{\mathbf{Y}}, \mathbf{Y}) = \frac{1}{Z_0} \sum_{i=1}^{n'} \sum_{j=1}^{t'} \frac{|Y_{ij} - \hat{Y}_{ij}|}{|Y_{ij}|} \mathbf{1}\{|Y_{ij}| > 0\}, \quad (12)$$

where $Z_0 = \sum_{i=1}^{n'} \sum_{j=1}^{t'} \mathbf{1}\{|Y_{ij}| > 0\}$.

(iii) **SMAPE:** Symmetric Mean Absolute Percent Error is defined as follows,

$$\mathcal{L}_s(\hat{\mathbf{Y}}, \mathbf{Y}) = \frac{1}{Z_0} \sum_{i=1}^{n'} \sum_{j=1}^{t'} \frac{2|Y_{ij} - \hat{Y}_{ij}|}{|Y_{ij}| + |\hat{Y}_{ij}|} \mathbf{1}\{|Y_{ij}| + |\hat{Y}_{ij}| > 0\}, \quad (13)$$

where $Z_0 = \sum_{i=1}^{n'} \sum_{j=1}^{t'} \mathbf{1}\{|Y_{ij}| + |\hat{Y}_{ij}| > 0\}$.

(iv) **MAE:** Mean Absolute Error is defined as follows,

$$\mathcal{L}_{mae}(\hat{\mathbf{Y}}, \mathbf{Y}) = \frac{1}{n't'} \sum_{i=1}^{n'} \sum_{j=1}^{t'} |Y_{ij} - \hat{Y}_{ij}| \quad (14)$$

(iv) **RMSE:** Root Mean Squared Error is defined as follows,

$$\mathcal{L}_{rmse}(\hat{\mathbf{Y}}, \mathbf{Y}) = \sqrt{\frac{1}{n't'} \sum_{i=1}^{n'} \sum_{j=1}^{t'} (Y_{ij} - \hat{Y}_{ij})^2}. \quad (15)$$

D.1 Linear Generative Model and Analogy to Mixed Linear Regression

For the sake of completeness, we define a linear generative model for our time-series setting under which we expect our algorithm to recover the true parameters. In the second half of this

section, we will relate this model to the simplified mixed linear regression problem, under which we formally prove our guarantees.

We will consider an auto-regressive lag of d . That is, any data point at a given time can depend only on quantities no more than d time steps in the past. We consider a dataset with n time series and T time points. The following process selects the local autoregressive parameters for each time series $i \in [n]$:

$$\mathbf{c}^*(i) \sim \text{Categorical}(\pi_1, \dots, \pi_k), \quad \text{and} \quad (16a)$$

$$\theta_i \mid \mathbf{c}^*(i) \sim \text{N}_d(\bar{\theta}_{\mathbf{c}^*(i)}, \nu^2 I_d), \quad (16b)$$

where Categorical and N_d denote the Categorical and d -dimensional Gaussian distributions respectively.

This means that the time series i is first randomly assigned into one of k clusters $\mathbf{c}^*(i)$. Based on the cluster, the local autoregressive parameters of the time series are drawn from the $\mathbf{c}^*(i)$ -th component of a Gaussian Mixture model in \mathbf{R}^d . The evolution of the time series is then given as follows:

$$x_i^{(s)} = \theta_i^\top x_i^{(s-d:s-1)} + \sum_{\substack{j \neq i \\ \mathbf{c}^*(i) = \mathbf{c}^*(j)}} \gamma_{ij}^\top x_j^{(s-d:s-1)} + \varepsilon_i^{(s)}, \quad (17)$$

for $s \in \{d+1, \dots, T\}$. Here, $\gamma_{ij} \in \mathbf{R}^d$ are parameters that govern how time series i depends on the past of time series j , only if both of them belong to the same cluster. This essentially implies that apart from the dependence on its own past, a time series can depend on the past of all other time series in the same cluster. Moreover the clustering is defined by closeness with respect to the local autoregressive parameters. From Equation (17), we see that the values of a time series do not depend on those from clusters that the corresponding time series does not belong to. This is a reasonable assumption in real-world multivariate time-series settings, where each time series would only depend on a few related time series.

Relation to MLR: The mixed linear regression problem is an i.i.d analogue of the linear generative model presented above. Each time-series can be thought of as a scalar regression problem, where each data-point in the MLR problem corresponds to the target being the future time-point and the covariates being the past d time-points, i.e

$$(x_i^{(j)}, y_i^{(j)}) \sim (x_i^{(s_j-d:s_j-1)}, x_i^{(s_j)}). \quad (18)$$

where s_j corresponds to the blocks separated by the mixing time, defined in Section 3. Time-series that come from the same cluster would have θ_i 's from the same component of the mixture in MLR model defined in Section 4. The time-series in the same cluster will have further VAR dependencies on each other as captured by γ coefficients in the MLR model.